Pure Appl. Chem., Vol. 82, No. 8, pp. 1691–1699, 2010.
doi:10.1351/PAC-CON-09-10-39

Electrochemical dissolution behavior of conductive TiC_xO_{1-x} solid solutions*

Shuqiang Jiao, Xiaohui Ning, Kai Huang, and Hongmin Zhu‡

School of Metallurgical and Ecological Engineering University of Science and Technology Beijing, Beijing, 100083, China

Abstract: Conductive TiC_xO_{1-x} solid solutions were prepared by carbothermic reduction of titanium dioxide. Studies were focused on the possibility of electrochemically dissolving TiC_xO_{1-x} in NaCl–KCl molten salt. The tail-gas from the anode was monitored during the electrolysis. It was discovered that carbon monoxide (CO) or carbon dioxide (CO_2) gases were generated, with the process being dependent upon the consumption of the TiC_xO_{1-x} solid solution anode materials. Furthermore, a series of electrochemical methods was used to investigate the valence state of titanium ions dissolved into molten salt when electrolyzing TiC_xO_{1-x} solid solutions. A significant result was that titanium ion species dissolved from the TiC_xO_{1-x} solid solutions, and this is changed between Ti^{2+} and Ti^{3+} depending on the electrochemically dissolving potentials. The significant result discovered in this paper will be potentially beneficial in the preparation of high-purity titanium by electrorefining TiC_xO_{1-x} solid solutions.

Keywords: anodes; electrochemical dissolution; electrolysis; solid solutions; titanium.

INTRODUCTION

Titanium, the fourth most abundant element in the earth's crust, is endowed with an excellent strength-to-weight ratio and the ability to withstand high temperatures and corrosive environments. These characteristics make titanium eminently suitable to use in the aerospace and marine industries and in harsh chemical environments.

The primary titanium metal, sponge titanium, is commonly produced by a process invented by Dr. Kroll in the 1940s [1]. The Kroll process is a batch method including two steps: the conversion from titanium oxide to titanium tetrachloride; and the reduction of titanium tetrachloride by magnesium metal. Unfortunately, the high cost of the Kroll process inhibits its widespread use.

For the above reason, since the early 1970s, research in titanium metallurgy has been directed toward developing a continuous process to produce high-purity titanium at low cost. Many alternative methods have been investigated. Electrolysis, involving the extraction and preparation of pure metal from ore using an electrolytic process, is considered a promising method for titanium metallurgy.

Early work was done in chloride and fluoride melts through feeding Ti^{4+}. A three-step reduction of Ti^{4+} to metal, $Ti^{4+} \rightarrow Ti^{3+} \rightarrow Ti^{2+} \rightarrow Ti$, is well known as the reduction mechanism [2–9]. The current efficiency was low, while sludge formation occurred. The difficulties are most likely related to the chemical disproportion reaction of Ti^{2+} and Ti^{3+}. High-purity metal can be electrodeposited on the cathode on the condition that most titanium ions are Ti^{2+} in the melt.

*Paper based on a presentation on the "Synthesis and Mechanism" theme at the 42nd IUPAC Congress, 2–7 August 2009, Glasgow, UK. Other Congress presentations are published in this issue, pp. 1569–1717.

‡Corresponding author

Recently, direct electrolysis from TiO_2 [10–14] or similar methods [15,16] have been presented extensively, with the most representative methods described below.

FFC CAMBRIDGE PROCESS

In 2000, Chen et al. reported a new process in which TiO_2, a semiconductor in the solid state, was electrochemically reduced directly to form metallic titanium, in molten $CaCl_2$ [10]. This new process was named the FFC Cambridge process. In the oxide electrolysis process, TiO_2 serves as the cathode and is reduced in an electrolyte of molten $CaCl_2$. The studies revealed that oxygen could be electrochemically removed from solid titanium oxide pellets, with titanium metal being ultimately formed at the cathode. A flowchart for this process is shown in Fig. 1, and it is noticeable that this process is comparatively less complex than the Kroll process. The overall series of cathodic reactions was ascertained to be [11–14]

$$5TiO_2 + CaO + 2e- = Ti_4O_7 + CaTiO_3 + O^{2-} \quad (1)$$

$$4Ti_4O_7 + CaO + 2e- = 5Ti_3O_5 + CaTiO_3 + O^{2-} \quad (2)$$

$$3Ti_3O_5 + CaO + 2e- = 4Ti_2O_3 + CaTiO_3 + O^{2-} \quad (3)$$

$$2Ti_2O_3 + CaO + 2e- = 3TiO + CaTiO_3 + O^{2-} \quad (4)$$

$$3TiO + CaO + 2e- = 2Ti + CaTiO_3 + O^{2-} \quad (5)$$

Finally, the reduction of calcium titanate and the removal of dissolved oxygen from the titanium are as follows:

$$CaTiO_3 + 2e- = Ti + CaO + O^{2-} \quad (6)$$

$$O_{(Ti)} + 2e- = O^{2-} \quad (7)$$

The corresponding anodic reaction is

$$C + 2O^{2-} = CO_2 + 4e \quad (8)$$

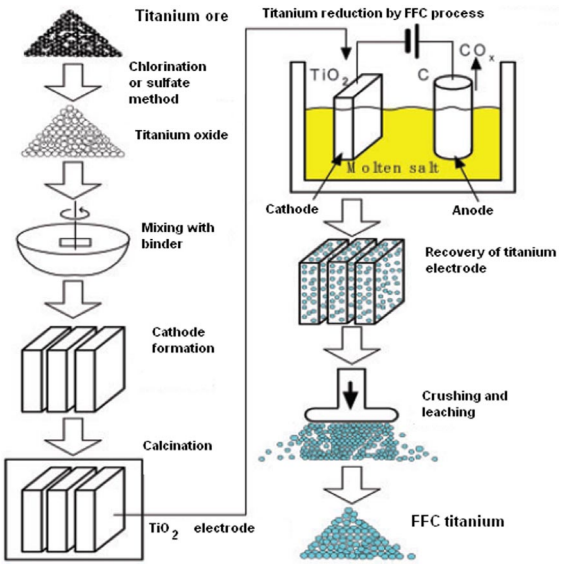

Fig. 1 Flowchart for the FFC Cambridge process [14].

ONO AND SUZUKI (OS) PROCESS

This process was developed by Ono and Suzuki and uses calcium to reduce TiO_2 [15,16].

$$2Ca + TiO_2 = 2CaO + Ti \quad (9)$$

A simple schematic of the cell used in the OS process is shown in Fig. 2. The process based upon the electrochemical deposition of calcium and the subsequent reduction of TiO_2 is being piloted. In the OS process, the generation of calcium and the reduction of TiO_2 occurred in the same vessel. With the container in direct contact with the cathode, the arrangement is very similar to the FFC Cambridge process.

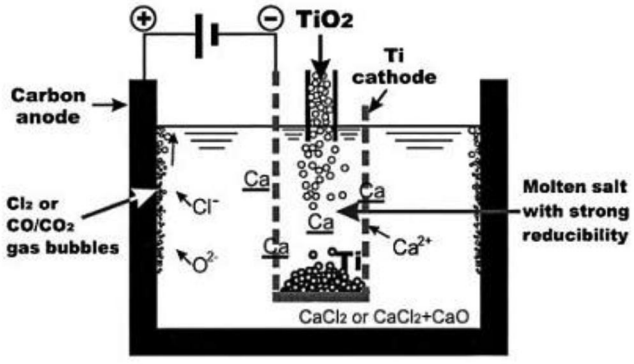

Fig. 2 Schematic of the cell used in the OS process [16].

MER PROCESS

MER Corporation developed a new process to produce titanium which commences with cost-affordable titania-rich feedstocks and a cheap source of carbon [17]. A schematic of the process is shown in Fig. 3. The composite anode contains a reduced TiO_2 compound, such as Ti_xO_y–C. Titanium ions are released into the electrolyte and are deposited as solid titanium at the cathode. A CO–CO_2 mixture is evolved at the anode. Indeed, MER has been awarded a DARPA contract for development of their process.

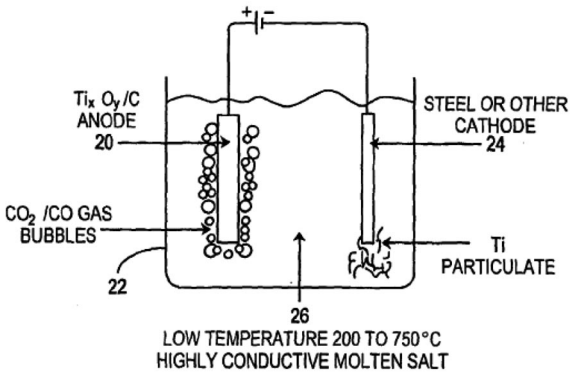

Fig. 3 Schematic diagram of the MER process [17].

USTB PROCESS

Another novel process for producing high-purity titanium has been developed by Zhu et al. at the University of Science and Technology Beijing (USTB), by electrorefining titanium oxycarbide solid solution [18]. A schematic of the USTB process is shown in Fig. 4. It is well known that high-purity titanium can be obtained on the cathode through electrorefining when titanium carbide (TiC) is used as a consumable anode [8]. In practice, however, carbon from the anode would be remaining in the electrolyte during electrolysis. In the USTB process, we have presented the investigation in eliminating remaining carbon by incorporating an oxide component into the anode. Titanium oxycarbide, for example, $TiC_{0.5}O_{0.5}$, which has high conductivity, can be utilized as an anode material, similar to the anodes used in aluminum electrowinning. When $TiC_{0.5}O_{0.5}$ was used as the anode in a molten salt bath, CO was evolved, with titanium leaving the anode as titanium ions and diffusing to the cathode before being deposited to form titanium with low oxygen content [19,20]. Titanium monoxide (TiO) and TiC form a series of solid solutions TiC_xO_{1-x}, where x can be in a wide range of 0~1. It was found that the solid solutions of this titanium oxycarbide series TiC_xO_{1-x} were all metallically conductive. Therefore, it is possible to use such solid solutions as anode material for titanium electrolysis. In this work, a series of investigations have been carried out to ascertain the mechanism of the electrochemical dissolution of TiC_xO_{1-x}. Also, during electrolysis, the content of CO, CO_2, and O_2 was monitored online. Moreover, titanium ions dissolving from the TiC_xO_{1-x} anode into the melt were analyzed by cyclic voltammetry and square-wave voltammetry.

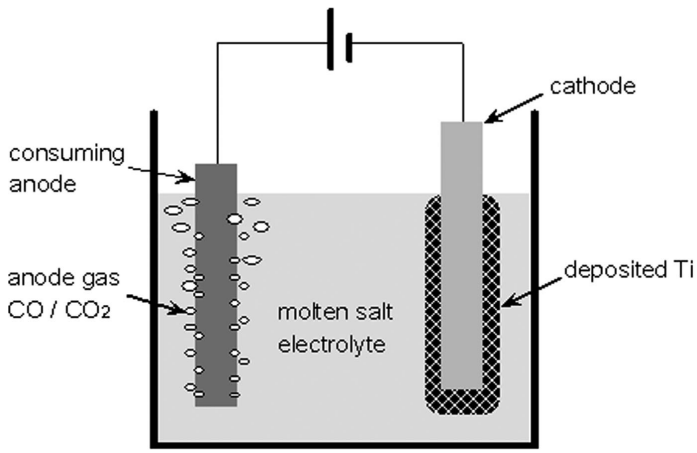

Fig. 4 Schematic diagram of the USTB process.

EXPERIMENTAL

TiC_xO_{1-x} was prepared using carbothermic reduction through reaction 10,

$$TiO_2 + (1 + 2x)C = TiC_xO_{1-x} + (1 + x)CO \quad (10)$$

The reactants were thoroughly mixed at stoichiometric proportions at room temperature, and then the mixture was pressed into a pellet of 3-mm diameter and 10-mm length. The pellet was subsequently sintered for 4 h at temperatures in a range between 1500 to 1700 °C under a vacuum of less than 100 Pa. The product structure was confirmed by X-ray diffraction (XRD), and the conductive efficiency was measured by four-probe method. This pellet had sufficient mechanical strength for making the thread. A stainless steel rod was used to connect with TiC_xO_{1-x} solid solution. The position of the anode was carefully adjusted in order to immerse only the TiC_xO_{1-x} into the electrolyte.

The electrolyte used was 50 wt % NaCl–KCl (reagent grade, Beijing Chemical Industries). The salts were pre-dried in an alumina crucible under vacuum at elevated temperatures (300 °C) for 4 h to remove moisture. All electrochemical experiments were conducted in a sealed vessel under a dry argon atmosphere at 750 °C.

The electrolysis and electrochemical experiments were performed using a potentiostat/galvanostat (EG&G PAR 263 A). A graphite rod with a 6-cm diameter served as the counterelectrode. The reference electrode was an Ag–AgCl electrode, which consisted of a silver wire (1-mm diameter) in contact with a solution of AgCl (4 wt %) in a NaCl–KCl molten-salt mixture, contained in a Mullite tube. The reference electrode was calibrated by a square-wave current method against the liberation of Cl_2 gas, with all potentials recorded with respect to the Cl_2–Cl^- potential. The potentiostatic electrolysis was carried out using conductive TiC_xO_{1-x} solid solutions as the anode.

The anodic gas was analyzed for the concentration of CO, CO_2, and O_2 on line with a resolution mass spectra (Hidden, SPR-30) and a high-sensitivity gas analysis instrument (Horiba analysis instrument industries) connected to the electrode tail by Swagelok tubing. Cyclic voltammetry and square-wave voltammetry experiments were performed under the same conditions as electrolysis. For those measurements, a 0.1-mm tungsten disk electrode was used as the working electrode.

RESULTS AND DISCUSSION

The $TiC_{0.5}O_{0.5}$ solid solution with a conductivity of 100 S cm^{-1} was found to electrochemically dissolve into the molten salt once an anodic potential was applied. Indeed, CO was evolved at the anode, and it was determined that the titanium formed titanium ions, dissolving into the molten salt and then diffused to the cathode, where it discharged to form high-purity titanium metal [19,20]. As aforementioned, a series of conductive TiC_xO_{1-x} solid solutions has been synthesized in this research. However, it is necessary to extend this research to all conductive TiC_xO_{1-x} solid solutions.

To investigate the product of the anodic reaction, various TiC_xO_{1-x} ($x = 0.50$, 0.33, and 0.20) solid solutions were used as anode materials, and a constant potential of –1.05 V (vs. Cl_2–Cl^-) was applied. Before electrolysis, the reactor was fully evacuated to form a vacuum and then charged by high-purity argon gas, to ensure that a baseline could be established for the anode gas concentration. The anode gas was analyzed before, during, and after the electrolysis by high-resolution mass spectra. The anode gas concentration profiles during electrolysis are presented in Fig. 5. From reference to Fig. 5, it is evident that the anode gas concentration profiles follow the potential step. When initiating electrolysis, after a few seconds delay, the anode gases concentration steeply rises. It also indicates that the anode gases generated during electrolysis depend on the anode material. It is clear that, upon the electrolysis of $TiC_{0.5}O_{0.5}$, only the CO concentration changes with regard to the potential step, with no concentration change noticeable for CO_2 and O_2 that is reproducible to previously published work [19,20]. An interesting result is presented in Figs. 5b,c, in that a significant amount of CO_2 is evolved when the anode materials contain a higher molar ratio of the oxygen component. However, there was still some CO detected even when the value of x was less than 0.33. During the electrolysis we did not see any change in oxygen concentration of the anode gas for the samples of TiC_xO_{1-x}, indicating that there was no oxygen generation. This indicates that it is kinetically preferred to form CO in TiC_xO_{1-x} electrolysis. Therefore, it can be deduced that this reaction mechanism corresponds with reaction 11.

$$TiC_xO_{1-x} \rightarrow Ti^{n+} + CO + CO_2 + ne \quad (11)$$

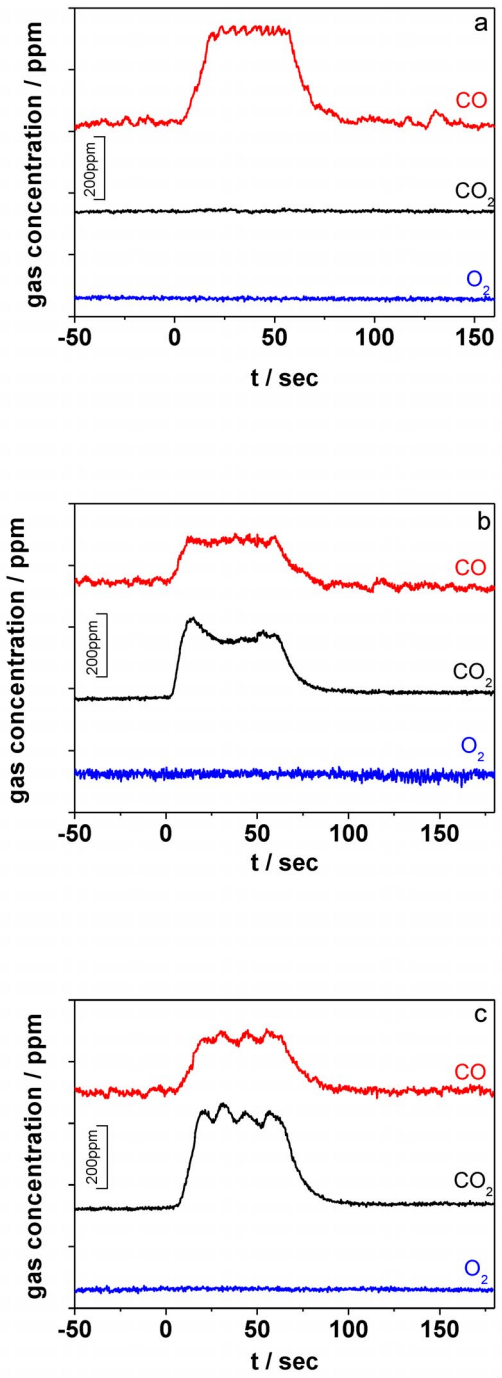

Fig. 5 Gas concentration profiles at different TiC_xO_{1-x} (x = 0.50 (a), 0.33 (b) and 0.20 (c)) under an applied anodic potential of –1.05 V (vs. Cl_2–Cl^-).

The conductive TiC_xO_{1-x} dissolves titanium ions directly into the melt while it is consumed. The species of the titanium ion dissolved in the molten-salt electrolyte during the electrolysis of the TiC_xO_{1-x} anode materials was also examined. The $TiC_{0.5}O_{0.5}$ anode was set at a potential of –0.65 V vs. Cl_2–Cl^- for 1 h, and then the molten salt was analyzed by cyclic voltammetry and square-wave voltammetry on a tungsten microdisk electrode. Figure 6 shows the corresponding cyclic voltammogram. It is noticeable that there is one cathodic peak (A), which is associated with two anodic peaks, (A') and (B'). Peak (A) is characteristic of the electrochemical reduction of titanium ion dissolved during $TiC_{0.5}O_{0.5}$ anode electrolysis. Peak (A', B') is associated again to the anode reaction from the metal to its ion, and then to a higher-valence ion. The square-wave voltammetry was also performed for the same electrode, due to its high sensitivity [21–23]. Figure 7 shows the typical current trace, compared with that before electrolysis. A peak appears at the potential around –1.62 V vs. Cl_2–Cl^-, corresponding to the reduction of titanium ion dissolved in the melt. Note that no such peak appears in the pre-electrolysis data because no titanium ions were present initially.

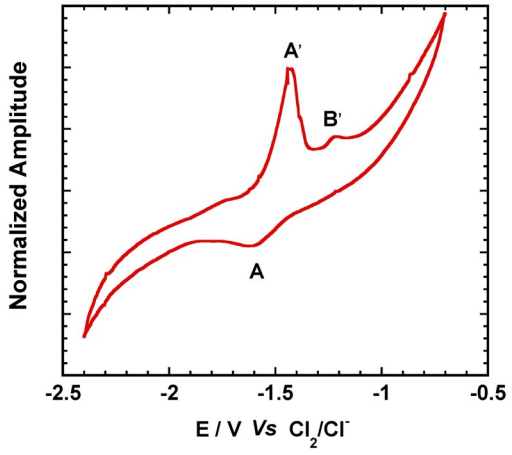

Fig. 6 A typical cyclic voltammogram for the measurment of titanium ions dissolved from $TiC_{0.5}O_{0.5}$ anode Sweep rate 0.1 V s^{-1}. (After 1 h electrolysis of $TiC_{0.5}O_{0.5}$ anode.)

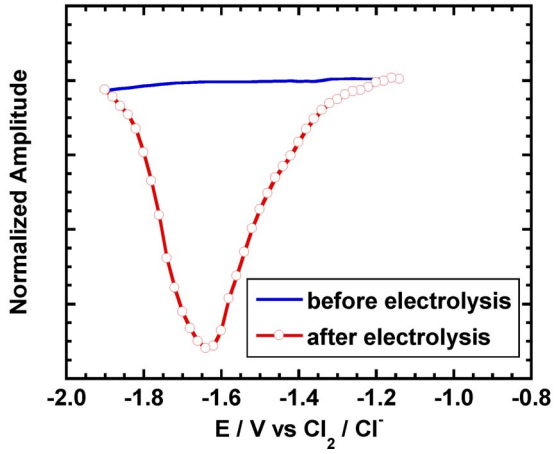

Fig. 7 Comparison of the square-wave voltammogram before and after electrolysis of $TiC_{0.5}O_{0.5}$, frequency 12.5 Hz. (After 1 h electrolysis of $TiC_{0.5}O_{0.5}$ anode.)

It is well known that titanium primarily ions can exist in multiple valence states; and consequently, titanium ions with different valence states could be dissolved into melt under various potentials. The amount of $TiC_{0.5}O_{0.5}$ was electrochemically dissolved into blank salt at potentials of –0.65, –0.45, and –0.25 V vs. Cl_2–Cl^-, respectively, with each dissolution of $TiC_{0.5}O_{0.5}$ lasting the same time of 1 h. Figure 8 presents the square-wave voltammograms recorded in the salts, after electrochemically dissolving $TiC_{0.5}O_{0.5}$ under various potentials.

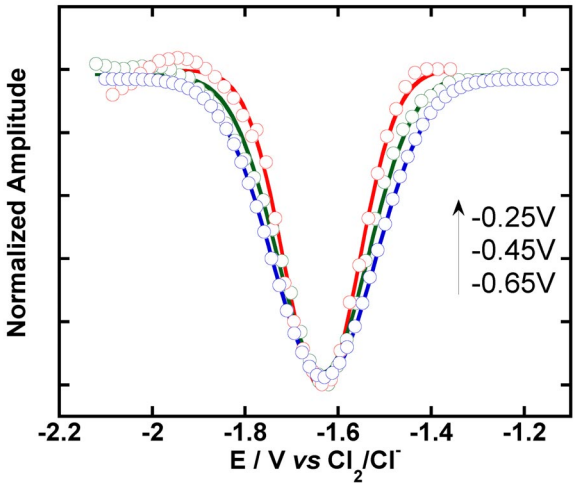

Fig. 8 Square-wave voltammograms of titanium ions detected in the salt after electrolysis of $TiC_{0.5}O_{0.5}$ at different potentials. (Dots for experimental data, solid lines for Gauss fitting.) (After 1 h electrolysis of $TiC_{0.5}O_{0.5}$ anode.)

The average exchange electron number of the electrochemical reduction of the titanium ions can be calculated from the half width of the peak $W_{1/2}$, by Gauss fitting (solid lines in Fig. 8), using the following eq. 12 [21–23].

$$W_{1/2} = 3.52\frac{RT}{nF} \tag{12}$$

Where n is the exchanging electron number, R is the ideal gas constant, T is the absolute temperature, and F is the Faraday constant.

Table 1 shows the $W_{1/2}$ by Gauss fitting and the exchanging electron number calculated. It is evident that the average exchanging electron number is changed from 2.1 to 2.8 with the increase of electrolysis potential. This implies that both Ti^{2+} and Ti^{3+} ions have been dissolved into the melt during electrolysis. Clearly, titanium valance states can significantly affect the cathodic current efficiency upon electrorefining TiC_xO_{1-x}. Increasing the amount of Ti^{3+} concentration can reduce the cathodic current efficiency. To produce metallic titanium on the cathode with high current efficiency, the electrorefining potential should be controlled appropriately. All of the results validate that eq. 11 aptly describes the electrochemical reaction occurring at TiC_xO_{1-x} anode.

Table 1 $W_{1/2}$ by Gauss fitting and exchanging electron number calculated.

	Electrolysis potential of TiC_xO_{1-x} (x = 0.5) (V vs. Cl_2–Cl^-		
	–0.65	–0.45	–0.25
$W_{1/2}$	0.140	0.127	0.105
n	2.1	2.3	2.8

CONCLUSION

Conductive TiC_xO_{1-x} solid solutions were prepared by carbothemic reduction of TiO_2. The TiC_xO_{1-x} anode can be electrochemically dissolved into NaCl–KCl molten salt under an applied potential. During electrolysis, CO and CO_2 gases were generated. The component of the anode gases depend upon the carbon and oxygen content in the TiC_xO_{1-x} anode material. A series of electrochemical methods was used to investigate the species of ions dissolved, and Ti^{2+} and Ti^{3+} ions were found to be the dissolving product at different electrolysis potentials.

ACKNOWLEDGMENTS

The authors wish to thank the National Basic Research Program of China (973 Program, 2007CB613301) for their financial assistance.

REFERENCES

1. W. J. Kroll. *Trans. Am. Electrochem. Soc.* **78**, 35 (1940).
2. F. R. Clayton, G. Mamantov, D. L. Manning. *J. Electrochem. Soc.* **120**, 1193 (1973).
3. D. Wei, M. Okido, T. Oki. *J. Appl. Electrochem.* **24**, 923 (1973).
4. T. Oishi, H. Kawamura, Y. Ito. *J. Appl. Electrochem.* **32**, 819 (2002).
5. F. Lantelme, K. Kuroda, A. Barhoun. *Electrochim. Acta* **44**, 421 (1998).
6. F. Lantelme, A. Salmi. *J. Electrochem. Soc.* **142**, 3451 (1995).
7. G. R. Stafford, T. P. Moffat. *J. Electrochem. Soc.* **142**, 3288 (1995).
8. B. N. Popov, M. C. Kimble, R. E. White. *J. Appl. Electrochem.* **21**, 351 (1991).
9. J. De Lepinay, P. Paillere. *Electrochim. Acta* **29**, 1243 (1984).
10. G. Z. Chen, D. J. Fray, T. W. Farthing. *Nature* **407**, 361 (2000).
11. D. J. Fray. *JOM* **53**, 27 (2001).
12. G. Z. Chen, D. J. Fray. In *Light Metals*, J. L. Anjier (Ed.), pp. 1147–1152, TMS, Warrendale (2001).
13. G. Z. Chen, D. J. Fray. *J. Electrochem. Soc. E* **149**, 445 (2002).
14. D. J. Fray. *Int. Mater. Rev.* **53**, 317 (2008).
15. K. Ono, R. O. Suzuki. *JOM* **54**, 59 (2002).
16. R. O. Suzuki, K. Ono, K Teranuma. *Metall. Mater. Trans. B* **34**, 287 (2003).
17. J. C. Withers, R. O. Loutfy. Patent WO 2005/019501.
18. H. M. Zhu, S. Q. Jiao, X. F. Gu. Patent CN1712571A.
19. S. Q. Jiao, H. M. Zhu. *J. Mater. Res.* **21**, 2172 (2006).
20. S. Q. Jiao, H. M. Zhu. *J. Alloys Compd.* **438**, 243 (2007).
21. L. Ramaley, M. S. Krause Jr. *Anal. Chem.* **41**, 1362 (1969).
22. M. S. Krause Jr., L. Ramaley. *Anal. Chem.* **41**, 1365 (1969).
23. J. H. Christle, J. A. Turner, R. A. Osteryoung. *Anal. Chem.* **49**, 1989 (1977).

